IEEE Access
Multidisciplinary | Rapid Review | Open Access Journal

Received August 28, 2020, accepted September 16, 2020, date of publication September 23, 2020, date of current version October 6, 2020.

Digital Object Identifier 10.1109/ACCESS.2020.3026077

Scheduling and Decoding of Downlink Control Channel in 3GPP Narrowband-IoT

PAVAN REDDY MANNE[1], SANTOSH GANJI[2], (Graduate Student Member, IEEE), ABHINAV KUMAR[1], (Senior Member, IEEE), AND KIRAN KUCHI[1], (Member, IEEE)

[1]Department of Electrical Engineering, IIT Hyderabad, Hyderabad 502285, India
[2]Electrical and Computer Engineering, Texas A&M University, College Station, TX 77843, USA

Corresponding author: Pavan Reddy Manne (ee14resch11005@iith.ac.in)

This work was supported by the 5G Testbed Project sponsored by the Department of Telecommunications (DoT), Government of India.

ABSTRACT Narrowband Internet of Things (NB-IoT) is a low power wide area network technology introduced by the 3rd Generation Partnership Project (3GPP). It is a derivative of the existing 3GPP Long Term Evolution (LTE) that will enable cellular service to a massive number of IoT devices. In comparison with LTE and 5G New Radio, the NB-IoT devices will be of low cost, low throughput, and delay-tolerant. The reduction in available bandwidth and introduction of repetitions for achieving wider coverage requires modified Narrowband Physical Downlink Control Channel (NPDCCH) search space design and decoding as compared to the LTE. Hence, in this paper, we first explain the NPDCCH physical layer procedures, along with the search space decoding. Unlike LTE, there is no channel feedback mechanism in NB-IoT. Therefore, we propose a novel resource mapping scheme for NPDCCH based on the uplink reference signals. We perform system-level simulations and analyze the impact of the proposed mapping for varying operating frequencies and channel conditions. Further, the NB-IoT devices have limitations on the battery power, and hence, the existing control channel schedulers cannot be reused for the NB-IoT scenario. Thus, we propose a novel scheduler for NPDCCH. We have also modified the current state-of-the-art algorithms to meet the NPDCCH constraints and compared them against the proposed scheduler. We derive bounds for such scheduling algorithms and show that the proposed scheduler additionally conserves up to 25% of the IoT device battery power. Through Monte Carlo simulations, we show that the proposed scheduler better achieves the various trade-offs between power consumption, search space utilization, and fairness as compared to the existing schedulers.

INDEX TERMS Aggregation level, blind decoding, Long Term Evolution (LTE), Narrowband Internet of Things (NB-IoT), schedulers, search space allocation.

I. INTRODUCTION

Narrowband Internet of Things (NB-IoT) has been introduced by the 3rd Generation Partnership Project (3GPP) in Release 13 [1]. It enables cellular service to ultra-low-cost IoT devices, which are delay-tolerant and operate at low data rates. NB-IoT provides wide signal coverage to a massive number of IoT devices. The industrial-IoT applications like smart metering, connected industrial appliances, animal/object tracking, and environmental monitoring are some key use cases of NB-IoT [2]. From Release 13 to 15, many enhancements have been specified by 3GPP for the NB-IoT. The NB-IoT standardization is expected to evolve and co-exist with 5G-New Radio as part of the industrial-IoT feature in future releases of 3GPP. The NB-IoT requires a bandwidth of 180 KHz and is deployable in three modes of operation, namely Standalone, Guard Band, and In-Band mode. In the Standalone mode, NB-IoT can operate on any Global System for Mobile communication (GSM) carrier with a bandwidth of 180 KHz. For the In-band mode, the NB-IoT is operated using a single physical resource block of LTE. In the Guard Band mode, the NB-IoT uses the guard band of LTE for allocating the resources. In all the three modes, NB-IoT operates with one resource block per subframe. In the Standalone and Guard Band modes, the entire resource block is available for NB-IoT, whereas, in the In-band mode, the first three symbols of the resource block are occupied by LTE [3]. For every mode of operation in the NB-IoT, there exist three physical downlink channels that are Narrowband Physical Broadcast Channel (NPBCH),

The associate editor coordinating the review of this manuscript and approving it for publication was Adnan Shahid.

This work is licensed under a Creative Commons Attribution 4.0 License. For more information, see https://creativecommons.org/licenses/by/4.0/

Narrowband Physical Downlink Control Channel (NPDCCH), and Narrowband Physical Downlink Shared Channel (NPDSCH). In this work, we focus on the NPDCCH for all the three modes of operation of NB-IoT.

The base station transmits Downlink Control Information (DCI) to the NB-IoT device in the NPDCCH. The NB-IoT device searches for the DCI within the designated search spaces, i.e., time-frequency resources in the NPDCCH. An NB-IoT device cannot establish a communication link with the network without decoding the DCI. In NB-IoT, the DCI is repeated over a large number of subframes to ensure successful decoding even in poor signal coverage. NB-IoT devices have cost and battery power constraints. Hence, an NB-IoT device cannot perform computations equivalent to a User Equipment (UE) in the traditional Long Term Evolution (LTE) systems for decoding the DCI. Thus, the search space design, scheduling of the devices in the search space, and DCI decoding in NB-IoT have to be different from LTE. In LTE, a base station allocates repetitions for a UE based on its channel feedback. However, NB-IoT has no provision for such a channel feedback [1]. Hence, NB-IoT requires a new mechanism for the allocation of these repetition levels. Unlike LTE, the control channel region in NB-IoT spans across subframes and has possibly 2048 configurations. As per 3GPP specifications [4], in an NPDCCH search space, at most eight NB-IoT devices can be scheduled. However, all the active NB-IoT devices try to decode this search space expecting a DCI. Thus, the NPDCCH scheduler should consider the power consumption of the IoT devices, minimize the resource wastage, and achieve fairness in scheduling. All these constraints and limitations make the NPDCCH scheduler design a challenging problem that has not been yet addressed in the existing literature. These are the key motivations for this work. In [5], we have presented the design rationale and search space allocation for NB-IoT. As compared to [5], the novel contributions of this paper are as follows.

- This is the first work to propose a mapping of repetition levels in NPDCCH to each NB-IoT device based on its uplink reference signals.
- We analyze the performance of the proposed novel mapping procedure for various channel configurations and operating band scenarios. We perform a sensitivity analysis of the proposed procedure for best-worst case scenarios.
- We frame the search space allocation as an optimization problem. We then propose schedulers for this search space allocation in NPDCCH. Bounds on performance of the proposed schedulers are derived.
- Through extensive numerical results, we show that the proposed schedulers achieve suitable trade-offs between various performance metrics.

The rest of the paper is organized as follows. In Section II, we present related work in the literature. The decoding of NPDCCH is explained in detail in Section III. The novel repetition level mapping for NB-IoT devices is proposed in Section IV. In Section V, the proposed search space schedulers, and performance metrics are presented. The simulation model and numerical results are discussed in Section VI. Some concluding remarks and possible future works are discussed in Section VII. For ease of reading a list of acronyms is presented in Table 1.

TABLE 1. List of acronyms.

3GPP	3rd Generation Partnership Project
AL	Aggregation Level
BD	Blind Decode
BLER	Block Error Rate
CDF	Cumulative Distribution Function
CQI	Channel Quality Indicator
CRC	Cyclic Redundancy Check
CSS	Common Search Space
DCI	Downlink Control Information
FDD	Frequency Division Duplex
ITU	International Telecommunication Union
LTE	Long Term Evolution
MTC	Machine Type Communications
NB-IoT	Narrowband-Internet of Things
NCCE	Narrowband Control Channel Elements
NPBCH	Narrowband Physical Broadcast Channel
NPDCCH	Narrowband Physical Downlink Control Channel
NPDSCH	Narrowband Physical Downlink Shared Channel
NPSS	Narrowband Primary Synchronization Signal
NSSS	Narrowband Secondary Synchronization Signal
OFDMA	Orthogonal Frequency Division Multiple Access
PDCCH	Physical Downlink Control Channel
QoS	Quality of Service
RE	Resource Element
RNTI	Radio Network Temporary Identifier
SINR	Signal-to-Interference plus Noise power Ratio
SNR	Signal-to- Noise power Ratio
TDD	Time Division Duplex
UE	User Equipment
USS	UE-specific Search Space

II. RELATED WORK

A. ON PERFORMANCE EVALUATION OF CONTROL CHANNEL

A detailed description and performance evaluation of uplink and downlink physical channels of NB-IoT have been presented in [6]. In [7], authors have performed system-level simulations, analysed the system throughput and delay-tolerance in an NB-IoT system. In [8], authors have studied the maximum achievable data rates, and presented optimal power and rate allocation techniques for NB-IoT. In [6]–[8], a detailed explanation of NB-IoT design and physical layer procedures has been presented. In [9], a reinforcement learning-based framework to configure resources optimally for uplink in NB-IoT has been presented. In [10], authors have proposed an uplink link-adaptation scheme for the IoT devices in an NB-IoT network. However, the constraints for uplink resource allocation are entirely different

from downlink, and hence, these algorithms cannot be used for NPDCCH. In [11], [12], the link-level simulation results for various physical layer channels of enhanced MTC (eMTC) have been presented. In [13], the performance evaluation of enhanced downlink control channel for MTC has been presented. In [14], a detailed explanation of physical layers and their performance for eMTC of Release 13 has been presented. However, a suitable scheme for mapping repetition levels for control channel in NB-IoT has not been considered in the existing literature. Hence in this paper, we present the link level simulation results for the NPDCCH and then propose a novel mapping of repetition levels to the IoT devices using the uplink channel conditions.

B. ON SCHEDULING OF THE DEVICES IN CONTROL CHANNEL

In [15], several possible scheduling algorithms for LTE-PDCCH have been discussed. Further, considering the joint effect of random access procedure and PDCCH, a novel scheduling algorithm has been proposed in [15]. Based on the simulation results, it has been shown that the proposed scheduling algorithm improves QoS provisioning for real-time traffic. In [16], a new scheduling algorithm for LTE-PDCCH using a linear transformation matrix has been presented. The resource allocation problem for LTE-PDCCH has been formulated as a set packing problem and has been solved using a linear programming based approach in [17]. In [18], several possible scheduling algorithms for LTE-PDCCH have been proposed. These algorithms include sorting the users based on aggregation levels and shuffling the sorted users for resource allocation. In [19], novel random access mechanisms have been discussed for the smart meters deployed under the LTE network. The authors have proposed a technique that combines both contention and non-contention based methods. Through system-level simulations, the authors have validated the proposed methods against the 3GPP standard. In [20], considering the aggregation levels of various UEs, several downlink control channel scheduling algorithms have been proposed. The repetition levels are absent in LTE PDCCH. Whereas, in NPDCCH, the varying repetition levels result in variable search space length. Hence, these LTE schedulers cannot be used directly in the context of NPDCCH. In [21] and [22], the performance of the downlink control channel in NB-IoT has been evaluated. However, the authors' have assumed a fixed search space length while evaluating NPDCCH resource allocation. The choice of the search space length has a significant impact on the resource utilization, power consumption of the IoT devices, and has not yet been addressed in the literature. Thus, we propose an optimized search space scheduler for NPDCCH in this paper. Next, we present the decoding of NPDCCH in detail.

III. DECODING OF NARROWBAND PDCCH

Downlink control information (DCI) is transmitted in the NPDCCH. The DCI block is repeated to achieve a specific size called aggregation level (AL) and is transmitted in a pre-defined set of subframes called as search space. In NPDCCH, the scheduling of DCIs is done in units of Narrowband Control Channel Elements (NCCEs). A detailed description of the DCI, ALs, NCCEs, search space, and NPDCCH receiver structure as per 3GPP specifications [3], [4], [23] has been presented in [5]. Readers unfamiliar with the NPDCCH design and structure are suggested to read [5].

TABLE 2. The UE-specific search space and the corresponding blind decodings.

$R^{\max}$	R	Format 0	Format 1	BDs
1	1	{0},{1}	{0,1}	3
2	1 2	{0},{1} –	{0,1} {0,1}	7
4	1, 2, 4	–	{0,1}	7
≥ 8	$\frac{R^{\max}}{8}, \frac{R^{\max}}{4}, \frac{R^{\max}}{2}, R^{\max}$	–	{0,1}	15

{x}– UE has to monitor NCCEx for DCI.
{x,y}– UE has to monitor NCCEx and NCCEy for DCI.

The repetition (R) and $R^{\max}$ define the subframe configuration for NPDCCH search space [4]. The $R^{\max}$ defines the number of valid subframes that a UE has to monitor for decoding DCI. The R defines the repetition, and UE has to blindly decode (BD) every R valid subframes from the start till the end of the search space. The various permissible values of $R^{\max}$, R, and BDs, for the two NPDCCH formats of UE-specific Search Space (USS) are presented in Table 2 [4]. *Note that each user is allocated a candidate set of R and AL in a search space*.

A. TIMING OF NPDCCH

Fig. 1 depicts the timing of NPDCCH and the respective NPDSCH decoding. NPBCH is present in the first subframe of every radio frame. Narrowband Primary Synchronization Signal (NPSS) occupies every sixth subframe of the radio frame. Narrowband Secondary Synchronization Signal (NSSS) occurs alternatively in the tenth subframe. NPDCCH and NPDSCH are present in the rest of the subframes.

Fig. 1 considers a search space of $R^{\max} = 4$ and scheduling of three NB-IoT devices. Even though NPDCCH search space starts at t = 2 ms, for an NB-IoT device D2 to start decoding, a minimum of one complete subframe of data is required. Thus, the decoding process starts at t = 3 ms. Subframe 5 is not a valid subframe for NPDCCH, and hence, it is not a part of the search space. Since the search space is of length 4, only subframes 2, 3, 4, and 6 are valid. Search space ends at t = 7 ms, and there is an extra 4 ms time for completing the NPDCCH decoding procedure. A minimum of 4 ms gap is present between any two search spaces [4]. Based on the scheduling of the devices, D2 can decode the DCI at t = 5 ms. Even though D2 gets successful in decoding DCI by t = 5 ms, it has to wait until t = 11 ms to start decoding NPDSCH. Whenever a base station broadcasts the NPDCCH region,

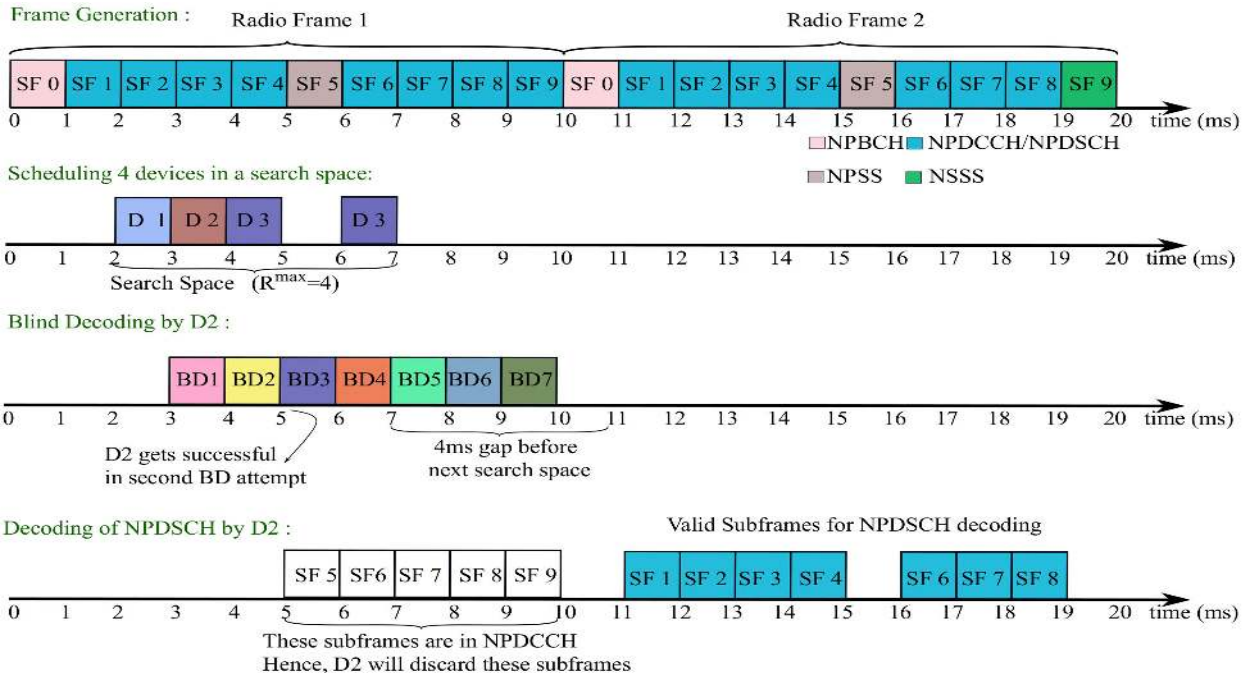

FIGURE 1. Timing diagram of NPDCCH decoding.

all the active devices try to decode the search space. A base station should accommodate the maximum number of devices in each search space to reduce the devices' power consumption. Further, the timing and search space constraints mentioned above will result in significant resource wastage if the scheduling is not done optimally. Next, we propose the mapping of repetition levels for NPDCCH.

IV. MAPPING OF REPETITION LEVELS

Typically, in cellular communication, the user conveys the channel quality to the base station by transmitting channel quality indicator (CQI) in the uplink. Based on the CQI, the base station can allocate the aggregation level to a UE. The transmission of CQI is absent in NB-IoT. Hence, we propose the following method for allocating the repetition level to an NB-IoT device.

A. MAPPING PROCEDURE

In the absence of CQI feedback, the uplink demodulation reference signal (DMRS) is the only information a base station has about the channel conditions of the NB-IoT device. NB-IoT devices periodically transmit DMRS in the uplink, and by decoding them, the base station can conclude on uplink channel conditions (SNR) for the NB-IoT device. The same can be used to approximate the downlink channel conditions for the NB-IoT device. Based on this approximated downlink channel conditions (SNR), the base station can have a mapping of repetitions and AL to BLER.

We present the performance of the NPDCCH for various repetition levels and transmit diversity schemes in Fig. 2, 3, as per the transmitter chain presented in [23] for NPDCCH.

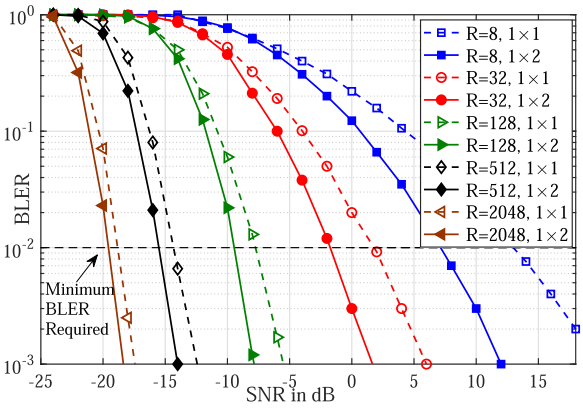

FIGURE 2. BLER of NPDCCH in standalone/guardBand modes.

The Table 3 presents simulation parameters considered for NPDCCH transmitter and receiver. The simulation has been carried for a bandwidth of 180 KHz and a sampling rate of 1.92 MHz over 10000 iterations. In each iteration, for a repetition level R, the block error rate (BLER) is calculated by repeating the rate-matched DCI block over R subframes. The BLER plots are generated for Standalone, Guardband, and In-band modes with one and two receive antennas, and various repetition levels. Fig. 2 presents BLER curves for Standalone and Guardband modes for both single and two receive antenna case. Fig. 3 presents BLER curves for In-band modes for both single and two antenna case. As mentioned in [5], the number of resources available for each aggregation level is lower in In-band mode. Thus, for a Standalone/Guardband mode, the received data can be soft combined over a large

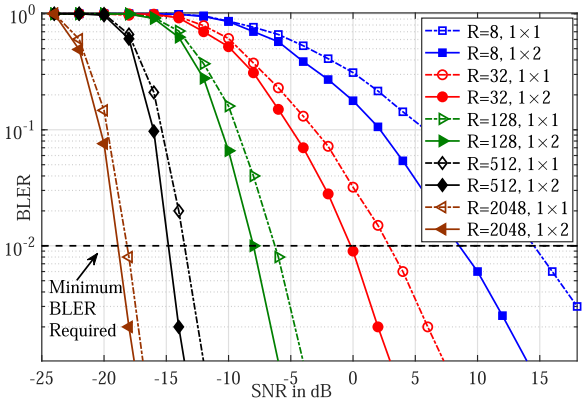

FIGURE 3. BLER of NPDCCH in in-band mode.

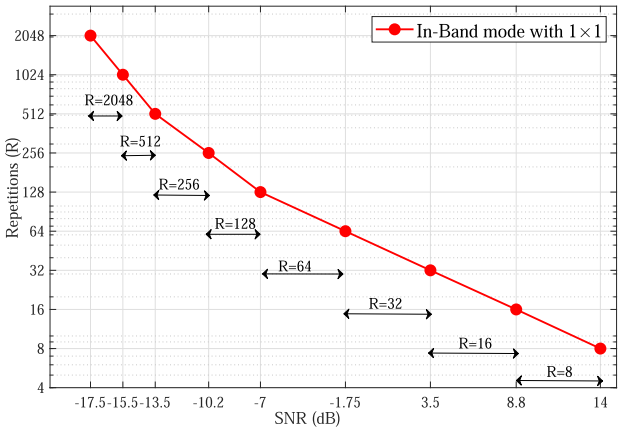

FIGURE 4. Mapping of SNR to R for in-band mode (1 tx, 1 rx).

TABLE 3. Link level simulation parameters.

Parameter	Value
Bandwidth	180 KHz (1 PRB)
Modes	Standalone/GB and In-Band
Sampling rate	1.92 MHz
Aggregation Level	2
DCI format	N1
Payload (w/o CRC)	23
No. of antennae (rx, tx)	(1, 1) and (1,2)
Propagation Condition	EPA5
Receiver	MRC
FEC	Tail-biting Convolution Code
Repetition ($R^{\max}$)	8, 32, 128, 512, 2048

TABLE 4. Mapping of SNR to R.

{R, AL}	Standalone/ GuarBand (1×1)	Standalone/ GuarBand (1×2)	In-Band (1×1)	In-Band (1×2)
{2048,2}	>-18 dB	>-19.5 dB	>-17.5 dB	>-18 dB
{512, 2}	>-14.5 dB	>-15.2 dB	>-13.5 dB	>-15 dB
{128, 2}	>-8 dB	>-9.5 dB	>-7 dB	>-8 dB
{32, 2}	>2 dB	>-2 dB	>3.5 dB	>-0.5 dB
{8, 2}	>13 dB	>7 dB	>14 dB	>8.5 dB

number of resource elements (REs) when compared to the In-band mode. Thus, for the same repetition level, the performance of Standalone/Guardband is better than that of the In-band mode. Also, the performance improves from a single receive antenna case to a two receive antenna case. This relative improvement is significant at smaller repetition values than at larger repetition values.

In [24], the mapping of SNR to the modulation and coding scheme of a user has been analyzed for various scenarios in the context of LTE. Motivated by this and the obtained simulation results, considering a BLER rate of 0.01 as a reasonable reference, we propose a mapping from SNR to repetition values in Table 4. A pictorial illustration of the mapping is presented in Fig. 4 for In-Band mode with 1 transmit and 1 receive antenna case. The BLER curves are obtained for various SNR values and repetition levels. For each repetition level curve, an SNR range is chosen such that the BLER is less than or equal to 0.01 and mapped, as shown in Fig. 4. Thus, a base station can perform a similar mapping for all possible combinations of repetition levels, aggregation levels, transmit diversity schemes, and channel models. Once the repetition levels are assigned to each NB-IoT device, they have to be scheduled in a feasible $R^{\max}$.

B. FEASIBILITY OF THE PROPOSED MAPPING PROCEDURE

In time division duplex (TDD) mode of operation, both uplink and downlink operate at the same carrier frequency. There is a minimal effect of using the signal to interference plus noise ratio (SINR) estimated in the uplink for allocating repetitions (R) to an NB-IoT device in the downlink. However, in the case of the frequency division duplex (FDD) mode of operation, the operating bands of uplink and downlink are different. The frequency selective nature and the dependency of path loss on the operating frequency [25] can cause differences in the uplink and the downlink SINRs. This difference in the uplink and downlink SINRs in the FDD mode of operation has an impact on the proposed mapping procedure. We analyze the sensitivity of the mapping procedure for the best and worst-case scenarios for different channel models as follows.

Given that the gap between the operating downlink and uplink frequencies has an impact on the SINRs, we consider the farthest and closest possible operating NB-IoT frequencies in Configuration A and Configuration B, respectively, as per 3GPP specifications [27]. The simulation parameters assumed are as per the International Telecommunication Union (ITU) specifications [26] and are presented in Table 5. In Table 5, the Configuration A has a maximum possible gap between the uplink and downlink operating frequencies. In this case, the uplink reference signals are comparatively less reliable for mapping repetitions in NPDCCH to an NB-IoT device, and hence, it is a worst-case scenario for

TABLE 5. System level simulation parameters.

Parameter	Value
Network Layout	7 cell sites, 3 sectors/site
Channel Model	UMa and UMi in 3GPP TR 38.901 [25]
Inter-site distance	500m (UMa) and 200m (UMi)
BS transmit power	44dBm (UMa) and 41 dBm (UMi)
NB-IoT Bandwidth	200 KHz
NB-IoT devices deployment	80% indoor, 20 % outdoor Randomly and Uniformly distributed over the area
BS Antenna Configuration $(M_b, N_b, P_b, M_{bg}, N_{bg})$	$(8, 1, 2, 1, 1)$
Device Antenna Configuration	2 antenna elements
BS antenna element gain	8 dBi
UE antenna element gain	0 dBi
NB-IoT Operating band	Configuration A (NB Band B66): $F_{DL} = 2200MHz$, $F_{UL} = 1710MHz$ Configuration B (NB Band B71): $F_{DL} = 691MHz$, $F_{UL} = 690MHz$
General Parameters	As per ITU M.2412 mMTC configuration [26]

mapping. The Configuration B has a minimum possible separation between the uplink and downlink frequencies, and thus, it is a best-case scenario. Note that M_b and N_b are the number of antenna elements at the base station with the same polarisation in vertical and horizontal directions, respectively, P_b is the polarisation, and M_{bg} and N_{bg} are the number of panels in vertical and horizontal directions, respectively. We perform system-level simulations with Urban-Macro and Urban-Micro channel models implemented as per 3GPP specifications [25]. For each NB-IoT device dropped in the sector, we measure the SINR at F_{DL} and F_{UL} as $SINR_{F_{DL}}$ and $SINR_{F_{UL}}$, respectively. We then calculate the absolute difference of the SINRs as $|SINR_{F_{UL}} - SINR_{F_{DL}}|$ for each device, and plot the cumulative distribution function (CDF) for the same over multiple realizations. In Fig. 5, with a 90% probability, the SINR difference is less than 2.5 dB in the best-case scenario, and it is less than 4.5 dB in the worst-case scenario. Note that in Fig. 4, on an average, the SINR difference between any two repetition levels is around 3 dB. Thus, in a worst-case scenario, with more than 0.9 probability, the proposed mapping would erroneously map to a repetition level next to the ideal repetition level. However, the base stations can be conservative and increase the repetition by one level to address this frequency selective nature of FDD.

Note that in TDD mode of operation, the proposed mapping procedure has a minimal impact on the repetition level allocation. Further, for the FDD mode of operation, in the absence of any direct information, the proposed mapping provides a close approximation for the repetition level allocation. Next, we present the proposed schedulers for NPDCCH.

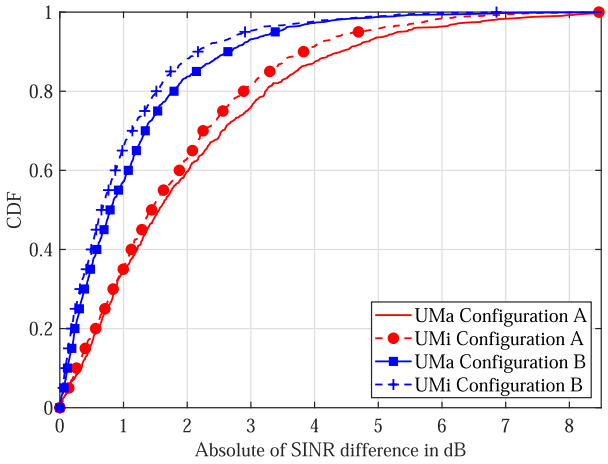

FIGURE 5. CDF of absolute SINR difference between DL and UL for different NB-IoT operating band configurations.

V. SEARCH SPACE ALLOCATION

The control channel schedulers allocate time and frequency resources to active users following a particular allocation model. The scheduler should determine the number of resources to be allocated to each user and signal all allocated users efficiently over NPDCCH. We initially formulate the search space constraints and define various metrics to evaluate the performance of the schedulers. Then, we propose a generalized NPDCCH search space scheduler, which provides flexibility in switching between the defined metrics. We extend the existing LTE schedulers based on the defined search space constraints and compare their performance with the proposed scheduler.

A. SEARCH SPACE ALLOCATION CONSTRAINTS

The search spaces are only allocated for active NB-IoT devices. A search space scheduler should assign the available search spaces to these active devices. This scheduling can be performed considering different strategies like prioritization of devices, reduction in delay, fairness, and maximizing the subframe utilization. We denote a search space in the allocation as S_i. $R_i^{\max}$ denotes the maximum possible size of a search space S_i. R_{ij} is used to denote the repetition level j. a_{ij} denotes the number of devices with repetition R_{ij} in ith search space and D_j denotes the number of devices requiring repetition R_{ij}. The scheduler must adhere to the following constraints as per 3GPP specifications [4].

$$S_i = \sum_{j=1}^{12} a_{ij} R_{ij} \leq R_i^{\max} \tag{1}$$

$$\sum_{i=1}^{N} a_{ij} \geq D_j, \quad \forall j = 1, \ldots, 12, \tag{2}$$

$$R_{ij} = 2^{j-1}, \quad \forall j \in \{1, \ldots, 12\}, \tag{3}$$

$$R_i^{\max}, R_{ij} \in \{1, 2, 4, \ldots, 2048\}, \tag{4}$$

$$a_{ij} = 0,$$

$$\begin{aligned} &\forall R_{ij} \notin \left\{R_i^{\max}, R_i^{\max}/2, R_i^{\max}/4, R_i^{\max}/8\right\} \\ a_{ij} \in &\{0, 1, 2, 4, 8\}, \\ &\forall R_{ij} \in \left\{R_i^{\max}, R_i^{\max}/2, R_i^{\max}/4, R_i^{\max}/8\right\} \end{aligned} \tag{5}$$

According to the constraint (1), the sum of the repetition levels of all the allocated devices in a search space should be less than or equal to the maximum possible size of that search space ($R_i^{\max}$). The sum of the devices allocated for each repetition level (R_{ij}) over all the search spaces should be greater than or equal to the number of devices requiring that repetition level (D_j), and the same is reflected in (2). The repetition level R_{ij} can take 12 possible values [4], as shown in (3). The constraint in (4) specifies that $R_i^{\max}$ and R_{ij} range from 1 to 2048 subframes. (5) specifies that in a search space, only four possible repetition levels are allowed [4].

Given D_j devices requiring a repetition level of R_{ij}, the allocation model can also consider some order or priority over the set of active devices. This prioritization can be based on the order of arrival of request, type of control information requested, or any other parameter.

A sample search space allocation is presented in Fig. 1. Although, a search space length of 4 is considered in Fig. 1, it can be of 1, 2, 4,..., 2048 subframes as mentioned in (4). In Fig. 1, in the search space with $R_1^{\max} = 4$, D1 and D2 take repetition of one subframe each ($R_{11} = R_1^{\max}/4, a_{11} = 2$) and D3 has repetition of two subframes ($R_{12} = R_1^{\max}/2, a_{12} = 1$). Both of these satisfy the constraint in (4), and $S_1 = a_{11}R_{11} + a_{12}R_{12} \leq R_1^{\max} = 4$ satisfies (1). Next, we discuss the various performance metrics considered in this work.

B. PERFORMANCE METRICS

We define the following performance metrics for NB-IoT control channel schedulers.

1) SEARCH SPACE UTILIZATION (χ)

For any search space allocation, there may exist leftover unallocated subframes in the search spaces. These unallocated subframes in a search space cannot be used for any other purpose and result in poor resource utilization. A good search space scheduler should minimize the number of unallocated subframes in the search spaces. We define the search space utilization χ as ratio of sum of the repetitions required by the devices (R_{req}) to the sum of the search spaces (R_{sch}),

$$\chi = \frac{R_{req}}{R_{sch}} = \frac{\sum_i S_i}{\sum_i R_i^{\max}}, \quad \chi \leq 1. \tag{6}$$

A larger value of χ indicates a better search space utilization.

2) FAIRNESS IN ALLOCATION (ν)

Let the priority order of each device i be $\tau_i : \tau_i \in \{1, 2, \ldots, N\}$. Let the actual order of the allocation from a search space scheduler for a device be $\tau_i^a : \tau_i^a \in \{1, 2, \ldots, N\}$. Note that if a search space scheduler follows the same priority order as the original τ_i's, we consider that scheduler as fair. However, this may not be possible due to the constraints in (1)-(5). Thus, we calculate the difference in priority order before and after allocation as,

$$\tau_i^d = \tau_i - \tau_i^a.$$

For a completely unfair case, the users are allocated exactly opposite priority order such that $\tau_i^d = \tau_i^w$, where, $\tau_i^w \in \{-(N-1), -(N-3), \ldots, (N-3), (N-1)\}$. We define fairness parameter (ν) as,

$$\nu = 1 - \frac{\sum_{i=1}^{N} (\tau_i^d)^2}{\sum_{i=1}^{N} (\tau_i^w)^2}, \quad 0 \leq \nu \leq 1.$$

where, $\nu = 1$ implies a fair scheduler that allocates the original priority order and $\nu = 0$ is the most unfair scheduler possible.

3) POWER CONSUMPTION (η)

Each active device belongs to a search space. Multiple devices can belong to the same search space. When a search space is broadcasted through RRC messages, all the active NB-IoT devices try to decode the search space. A search space can be scheduled for a minimum of one user with $R_{ij} = R_i^{\max}$ and a maximum of eight users each with $R_{ij} = R_i^{\max}/8$. If a search space has only one device scheduled and say it is of length 2048 subframes, then all the other devices try decoding it and fail. This results in significant power consumption by the NB-IoT devices. The net power consumption of the active devices for a scheduler is calculated as

$$P_c = \sum_i \left(N - \sum_{j=1}^{i} N_j\right) S_i, \tag{7}$$

where, N is the number of active devices and N_j is the number of devices scheduled in the jth search space. Then, power consumption ratio for a scheduler is defined as,

$$\eta = \frac{P_c}{P_w}, \quad 0 < \eta \leq 1. \tag{8}$$

where, P_c is the power consumed for a scheduler calculated using (7), and P_w is the power consumed in a worst-case scenario. In a worst-case scenario, every search space has only one device, and the devices are prioritized in decreasing order of their repetition. Thus, for any search space allocation, a smaller η is better and corresponds to less power consumption by NB-IoT devices. Next, we present the proposed schedulers considered in this work.

C. SEARCH SPACE SCHEDULERS

Search space schedulers handle user requests for control information and allocates them time-frequency resources. The proposed scheduler considered in this work is as follows.

1) PROPOSED SCHEDULER

Optimizing the power consumption (η) will have an impact on the search space utilization (χ), and vice-versa. We formulate the search space allocation as an optimization problem to achieve a minimum power consumption and a better search space utilization. Motivated by the approach followed in [28], a variable α is introduced to achieve a trade-off between both. Using (6), (7) and (8), the objective function of the proposed scheduler is defined as follows:

$$\min_{\{a_{ij}\}} \left(\frac{\alpha}{\chi} + (1-\alpha)\eta\right) = \sum_{i=1}^{N}\sum_{j=1}^{12} a_{ij}R_{ij}\left(\frac{\alpha}{R_{req}} + (1-\alpha)\frac{\sum_{k=1}^{i}(N-N_k)}{P_w}\right) \quad \text{s. t. (1), (2), (4), and (5).} \tag{9}$$

where, a_{ij} denotes the number of devices with repetitions R_{ij} in a search space i. Once the search spaces are determined, the devices are picked in the order of their priority. The variable α is introduced to achieve the trade-off between search space utilization (χ) and power consumption (η). With $\alpha = 0$, the objective function will optimize only power consumption while scheduling the devices. With increasing α, the priority of the optimization shifts from power consumption to search space utilization. When $\alpha = 1$, the objective function will schedule the devices to achieve maximum search space utilization. When $\alpha = 0.5$, the objective function considers both the parameters with equal priority and schedules the IoT devices. Thus, our proposed scheduler allows the industrial operator to choose the suitable trade-off based on their selection of α.

Considering the constraints on the NPDCCH mentioned earlier, we have modified the existing LTE schedulers in the literature and present them next for comparison.

2) BASELINE SCHEDULER

The baseline scheduler is a primitive scheduler that retains the priority order of the active users, i.e., NB-IoT devices are scheduled in the order of their arrival or based on a priority order preset by the network. Thus, the search space selected for each device $R_{ij} = S_i = R_i^{\max}$ resulting in the same repetition level as needed by the device. This allocation although fair ($\nu = 1$) and with maximum search space utilization ($\chi = 1$) requires more search spaces to schedule all the requests, i.e., it has larger η. It has been shown in [18], and [20], that prioritizing the UEs in LTE based on their aggregation level eases up scheduling. In the case of NB-IoT, through sorting, the devices can be grouped into search spaces. Thus, we next present several schedulers that are based on the sorting of the devices according to their repetition levels.

3) MAX-R_i

In *Max-R_i* scheduler, the base station sorts the devices in the descending order of the repetition level. The first device in the sorted list is picked, and all possible $R_1^{\max}$'s are computed. The subsequent devices in the list, until repetition level $R_1^{\max}/4$, are checked if they can be grouped with the current device in a single search space. The maximum possible number of such devices are then grouped into this search space without violating the constraints in (1)-(5). This process is repeated until all devices are scheduled. With *Max-R_i* scheduler the search space is under-utilized. Thus, we next propose the *Max-R_i Relaxed* scheduler.

4) MAX-R_i RELAXED

In this scheduler, the devices are sorted in the descending order of the repetition level. However, the selection of $R_1^{\max}$ is to ensure full search space utilization in comparison with the objective of the maximum possible number of devices that can be grouped into the search space for *Max-R_i* scheduler. This ensures that no unallocated subframes are left at the cost of lowering the number of users scheduled per search space. We also consider the ascending order of repetition level as the priority order to propose the following two schedulers.

5) MIN-R_i AND MIN-R_i RELAXED

Min-R_i and *Min-R_i Relaxed* schedulers are similar to *Max-R_i* and *Max-R_i Relaxed* schedulers except that the sorting of the active devices is performed in ascending order. In *Min-R_i*, the scheduler tries to group more devices in each search space, whereas in *Min-R_i Relaxed*, the scheduler also ensures that no resources are left un-allocated.

D. ANALYSIS OF THE PROPOSED SCHEDULER

We calculate the upper bound and lower bound on the performance gains that we achieve with the proposed scheduler. Motivated by the procedure followed in [29], [30], we consider the best and worst case scenarios for calculating the bounds on the performance gains.

In Lemma 1, we prove that the χ with the proposed scheduler is either the same or better than the remaining schedulers. We also quantify the maximum performance gain that we achieve with the proposed scheduler. Note that a larger value of χ is better and corresponds to a better search space utilization.

Lemma 1: Let $\chi_{\text{algorithm}}$ denote the search space utilization of a scheduling algorithm. Further, let $\chi_{\text{algorithm}}^{\text{best}}$, $\chi_{\text{algorithm}}^{\text{worst}}$ denote the search space utilization of the algorithm in the best and worst case scenarios, respectively. Then, for any configuration of NB-IoT device distribution, the following holds:

(i) $\chi_{\text{Proposed}|_{\alpha=1}} = \chi_{\text{Min-R}_i\text{relaxed}} = \chi_{\text{Max-R}_i\text{relaxed}} = \chi_{\text{Baseline}}$

(ii) $\chi_{\text{Proposed}|_{\alpha=1}} \leq 1.6\chi_{\text{Min}-\text{R}_i}^{\text{worst}} = 1.6\chi_{\text{Max}-\text{R}_i}^{\text{worst}}$

$\chi_{\text{Proposed}|_{\alpha=1}} \geq \chi_{\text{Min}-\text{R}_i}^{\text{best}} = \chi_{\text{Max}-\text{R}_i}^{\text{best}}$,

Proof:

(i) In the *Baseline* scheduler, the base station schedules only one device in each search space, and hence, there is no resource wastage. By definition in Section V-C5 and Section V-C4, respectively, *Min-R_i relaxed* and *Max-R_i relaxed* schedulers do not leave any subframe unallocated in a search space. When $\alpha = 1$, (9) becomes an objective function that ensures the total number of subframes in all the scheduled search spaces ($\sum_{i=1}^{N}\sum_{j=1}^{12} a_{ij}R_{ij}$) is equal to the total number of repetitions required by the devices (R_{req}). There is no resource wastage in all the above scenarios, and thus,

$$\chi_{\text{Proposed}|_{\alpha=1}} = \chi_{\text{Min-R}_\text{i}\text{relaxed}} = \chi_{\text{Max-R}_\text{i}\text{relaxed}} = \chi_{\text{Baseline}}.$$

(ii) Let D_j represent the number of NB-IoT devices requiring the repetition level R_j, and as per (4), $R_j \in \{1, 2, \ldots, 2048\}$. Then, for *Min-$R_i$* and *Max-$R_i$* schedulers the following holds:

a) For any R_j in (4), $D_j = 5$ forms the worst-case scenario of search space utilization for *Min-R_i* and *Max-R_i* schedulers. This is because, in this scenario, *Min-R_i* and *Max-R_i* schedule all 5 devices requiring R_j in a single search space of size $R_1^{\max} = 8R_j$. Thus, as per (6),

$$\chi^{\text{worst}}_{\text{Min-R}_\text{i}} = \chi^{\text{worst}}_{\text{Max-R}_\text{i}} = \frac{5}{8}.$$

Note that in this scenario, the proposed scheduler with $\alpha = 1$, schedules the devices in two search spaces with $R_1^{\max} = 4R_j$ and $R_2^{\max} = R_j$. Thus, as per (6),

$$\begin{aligned}\chi_{\text{Proposed}|_{\alpha=1}} &= 1,\\ \chi_{\text{Proposed}|_{\alpha=1}} &= \frac{8}{5}\chi^{\text{worst}}_{\text{Min-R}_\text{i}} = 1.6\chi^{\text{worst}}_{\text{Min-R}_\text{i}}\\ &= \frac{8}{5}\chi^{\text{worst}}_{\text{Max-R}_\text{i}} = 1.6\chi^{\text{worst}}_{\text{Max-R}_\text{i}}.\end{aligned}$$

b) For any R_j in (4), $D_j = 1$ forms the best-case scenario of search space utilization for *Min-R_i* and *Max-R_i* schedulers. In this scenario, the proposed scheduler with $\alpha = 1$, *Min-R_i*, and *Max-R_i* schedule the device in a single search space of size $R_1^{\max} = R_j$. Thus, there is no resource wastage.

$$\chi_{\text{Proposed}|_{\alpha=1}} = \chi^{\text{best}}_{\text{Min-R}_\text{i}} = \chi^{\text{best}}_{\text{Max-R}_\text{i}}.$$

This completes the proof of Lemma 1. ∎

In NB-IoT, the time-frequency resources are valuable. As shown in Lemma 1, the proposed scheduler achieves better search space utilization when compared to the other schedulers. It can accommodate more number of NB-IoT devices when compared to other schedulers, and thus, achieve better system capacity.

In Lemma 2, we prove that η with the proposed scheduler is always the same or lower than the remaining schedulers. We also quantify the maximum gain in power consumption that can be achieved by the proposed scheduler. Note that a smaller value of η is better and corresponds to lower power consumption by the devices.

Lemma 2: Let $\eta_{\text{algorithm}}$ denote the power consumption of a scheduling algorithm. Further, let $\eta^{\text{best}}_{\text{algorithm}}$, $\eta^{\text{worst}}_{\text{algorithm}}$ denote the power consumption of a scheduling algorithm in the best and worst case scenarios, respectively. Then, for any configuration of NB-IoT device distribution, the following holds:

(i) $\eta_{\text{Proposed}|_{\alpha=0}} \leq \eta^{\text{best}}_{\text{S}}$,
$\text{S}\in\{\text{Min-R}_\text{i},\text{Min-R}_\text{i}\text{relaxed},\text{Max-R}_\text{i},\text{Max-R}_\text{i}\text{relaxed},\text{Baseline}\}$

(ii) $\eta_{\text{Proposed}|_{\alpha=0}} \geq 2^{-11}\eta^{\text{worst}}_{\text{Max-R}_\text{i}} = 2^{-11}\eta^{\text{worst}}_{\text{Max-R}_\text{i}\text{relaxed}} = 2^{-11}\eta^{\text{worst}}_{\text{Baseline}}$

(iii) $\eta_{\text{Proposed}|_{\alpha=0}} \geq 0.75\eta^{\text{worst}}_{\text{Min-R}_\text{i}} = 0.75\eta^{\text{worst}}_{\text{Min-R}_\text{i}\text{relaxed}}$

Proof:

(i) With $\alpha = 0$, the proposed scheduler in (9) becomes an objective function that tries to schedule more number of devices in a search space. Thus, the number of devices scheduled will always be greater than or equal to that of the other schedulers. Hence, as per (7), power consumption P_c with the proposed scheduler is always less than or equal to that of the other schedulers. Thus,

$$\eta_{\text{Proposed}|_{\alpha=0}} \leq \eta^{\text{best}}_{\text{S}},$$
$$\text{S}\in\{\text{Min-R}_\text{i},\text{Min-R}_\text{i}\text{relaxed},\text{Max-R}_\text{i},\text{Max-R}_\text{i}\text{relaxed},\text{Baseline}\}.$$

(ii) Let O_j represent the order of scheduling of the NB-IoT devices that require repetition R_j. Then, for *Max-R_i, Max-R_i relaxed*, and *Baseline* schedulers, the configuration with $\{R_1 = aR, R_2 = R \text{ and } O_1 = 1, O_2 = 2\}$ forms the worst-case scenario for power consumption. In this scenario, the search spaces with the proposed scheduler are $R_1^{\max} = R$, $R_2^{\max} = aR$, whereas, with *Max-R_i, Max-R_i relaxed*, and *Baseline* schedulers, the search spaces are $R_1^{\max} = aR$, $R_2^{\max} = R$. Thus, as per (7), in case of the proposed scheduler $P_c = R$, whereas, for the other schedulers it is $P_c = aR$. The maximum possible value of a is 2048, and hence,

$$\begin{aligned}\eta_{\text{Proposed}|_{\alpha=0}} &= 2^{-11}\eta^{\text{worst}}_{\text{Max-R}_\text{i}} = 2^{-11}\eta^{\text{worst}}_{\text{Max-R}_\text{i}\text{relaxed}}\\ &= 2^{-11}\eta^{\text{worst}}_{\text{Baseline}}.\end{aligned}$$

(iii) Let D_j represent the number of NB-IoT devices that require repetition R_j. Then, for *Min-R_i* and Min-R_i relaxed schedulers, the configuration with $\{R_1 = R, R_2 = 4R, R_3 = bR \text{ and } D_1 = 1, D_2 = 1, D_3 = 1 \text{ with } b > 4\}$ forms the worst-case scenario for power consumption. In this scenario, the search spaces with the proposed scheduler are $R_1^{\max} = R, R_2^{\max} = 4R, R_3^{\max} = bR$, whereas, with the other schedulers, the search spaces are $R_1^{\max} = 8R, R_2^{\max} = bR$. Thus, as per (7), in case of proposed scheduler, $P_c = 6R$, whereas, in case of the other schedulers it

is $P_c = 8R$.

$$\eta_{\text{Proposed}|_{\alpha=0}} = \frac{6}{8}\eta^{\text{worst}}_{\text{Min}-\text{R}_\text{i}\text{relaxed}} = 0.75\eta^{\text{worst}}_{\text{Min}-\text{R}_\text{i}\text{relaxed}} = \frac{6}{8}\eta^{\text{worst}}_{\text{Min}-\text{R}_\text{i}} = 0.75\eta^{\text{worst}}_{\text{Min}-\text{R}_\text{i}}.$$

This completes the proof of Lemma 2. ■

Note that the power consumption of the NB-IoT devices while monitoring the paging during RRC idle mode and decoding of the search spaces in the RRC connected mode has a significant impact on the battery life. As presented in Lemma 2, the power consumption of the NB-IoT devices is comparatively low with the proposed scheduler. When compared to the next best scheduler, the proposed scheduler with $\alpha = 0$ additionally conserves up to 25% of the IoT device battery power. Hence, the proposed scheduler has a significant impact on the power consumption of devices in the NB-IoT system.

E. FEASIBILITY OF IMPLEMENTATION

The objective function proposed in (9) is an NP-hard problem. This is a well-investigated subject, and there are various standard algorithms in [31], [32] to implement the same. The complexity of the objective function is proportional to the number of repetition levels and the number of devices considered for scheduling. For a case of 12 repetition levels and 100 devices, [31] presents the computational time taken by various algorithms run on a normal Pentium III (1GHz) processor, and the average computational time taken is observed to be ten milliseconds. NB-IoT systems operate only on one resource block and allow repetition of data over 20 milliseconds for each IoT device. Thus, unlike legacy systems, between any two scheduling events, there is sufficient time for the base station to make scheduling decisions. Hence, there is a minimal impact of the computational time taken by the scheduler, considering that it achieves the suitable search space utilization, fairness, and power consumption of IoT devices.

VI. RESULTS AND ANALYSIS

To evaluate the proposed schedulers, Monte Carlo simulations were performed in MATLAB. AMPL is a programming language that solves the optimization problem for a given objective function and constraints [33]. For the proposed scheduler, AMPL and an interface with MATLAB are used for simulations. The objective function in (9) is substituted with the values of N and α for each scenario. This objective function along with the constraints (1)-(5) is passed on to the AMPL, and the scheduled information (the values of a_{ij} and R_{ij}) is obtained. Using these a_{ij} and R_{ij} values, power consumption, search space utilization, and fairness are calculated for each IoT device. Table 6 presents the parameters used for the simulation. Although all our performance metrics are independent of the number of users, we present results for 1000 NB-IoT devices. The repetition levels of the users were uniformly distributed over the various permitted levels.

TABLE 6. Simulation parameters.

Parameter	Value
Bandwidth	180 KHz (1 PRB)
Number of active devices	1000
Repetition Level of each device (R_{ij})	1, 2, . . ., 2048 subframes
Search Space (S_i)	1, 2, . . ., 2048 subframes
Distribution of R_{ij} in NPDCCH	Uniform distribution
Priority order (τ_i)	Order of arrival

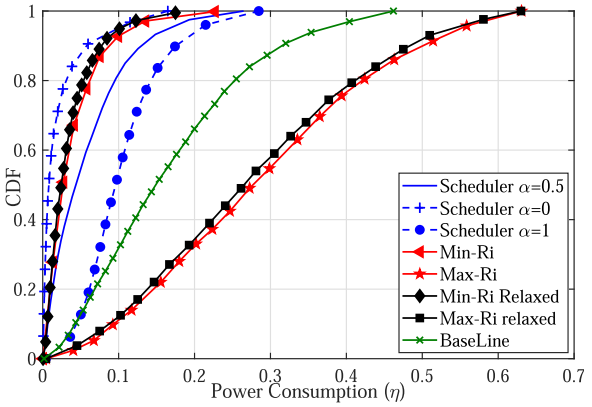

FIGURE 6. CDF of power consumption.

A. POWER CONSUMPTION (η)

In Fig. 6, the cumulative distribution function (CDF) plot for the power consumption ratio (η) is presented. The *Max-R_i* has the highest power consumption ratio. Since the scheduler picks the maximum possible search space length every time, a large number of devices try to decode this large search space length and fail. Thus, it results in a large power consumption ratio. The scheduler with the next largest η is *Max-R_i relaxed*. To maximize the search space utilization, comparatively smaller search space lengths are scheduled, and hence, it results in a lower power consumption ratio than *Max-R_i*. The baseline scheduler also has a high power consumption as it schedules the devices in the order of their arrival. Although, when compared to the *Max-R_i* and *Max-R_i relaxed*, it schedules the smaller search space lengths as well. Thus, the baseline scheduler has a comparatively lower η. In *Min-R_i*, the search spaces are alloted in increasing order. Hence, the power consumed by the devices decoding the smaller search space lengths will be less in *Min-R_i*. Thus, *Min-R_i* scheduler has low power consumption ratio. *Min-R_i relaxed* has much smaller search space lengths, and hence, has comparatively lower η.

Varying α, the priority of the proposed scheduler can be biased to either of η or χ. For $\alpha = 1$, since χ is more prioritized, it has comparatively more power consumption than that of $\alpha = 0.5$ or 0. Note that, the power consumption (η) is much lower than the *base scheduler*, *Min-R_i relaxed* and *Max-R_i relaxed*. For $\alpha = 0$, η is more prioritized, and

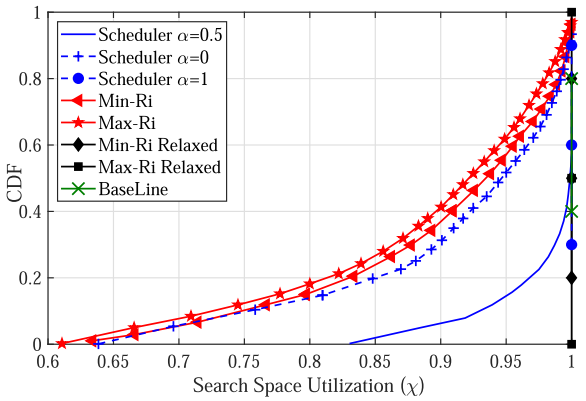

FIGURE 7. CDF of search space utilization.

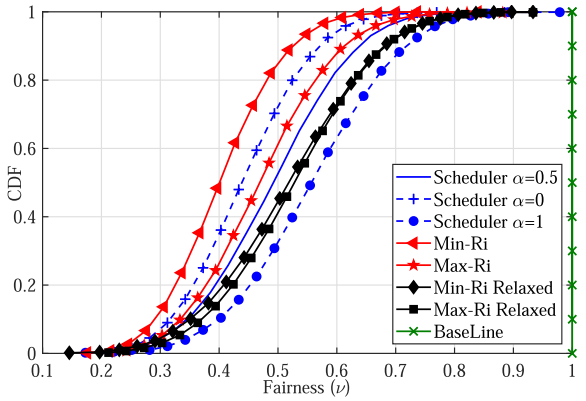

FIGURE 8. CDF of fairness in allocation.

the scheduler has the least power consumption among all the schedulers.

B. SEARCH SPACE UTILIZATION (χ)

In Fig. 7, the CDF of χ is presented for all the proposed schedulers. The *Min-R_i relaxed*, *Max-R_i relaxed*, and the *baseline scheduler* have complete search space utilization. *Min-R_i* has better utilization compared to *Max-R_i* as the scheduling is performed starting from smaller values of search space size resulting in a lesser number of unallocated subframes in comparison with *Max-R_i*. Since $\alpha = 0$ is more biased to η, it has poor search space utilization, whereas $\alpha = 1$ has the best search space utilization with $\chi = 1$.

C. FAIRNESS IN ALLOCATION (ν)

Considering the order of request arrival as the order of priority, the CDF plot of ν for the various schedulers is shown in Fig. 8. Note that by design, the *baseline scheduler* is most fair. The fairness of *Min-R_i* is less than that of *Max-R_i* as it can allocate more number of users with low repetition levels irrespective of their priority order. This is because more number of devices are packed in every search space in *Min-R_i*, whereas, *Max-R_i* allocates the users with a larger repetition first, and hence, accommodates fewer devices in every search space. The relaxed schedulers do not accommodate out of turn devices and result in scheduling less number of devices every time. Thus, the relaxed schedulers are more fair compared to their non-relaxed versions. When $\alpha = 0$, the number of devices allotted in a search space by the proposed scheduler is more than that of $\alpha = 0.5$ and 1. Hence, comparatively, it schedules more unfair devices every time. The proposed scheduler with $\alpha = 1$ has the best fairness next to the baseline scheduler.

D. TRADE-OFF BETWEEN PERFORMANCE METRICS

In Fig. 9, trade-off between various performance metrics is presented. For each scheduler, the mean of the power consumption (η), search space utilization (χ), and fairness (ν) across 1000 NB-IoT devices are calculated. These mean values are then scaled on a range of [0, 1] as follows,

$$\hat{\eta}_j = \frac{\eta_j - \eta_{min}}{\eta_{max} - \eta_{min}},$$

where, η_j is the power consumption for the scheduler type j, and η_{min} and η_{max} are the minimum and maximum power consumption values among all the schedulers. Similarly, the normalized values are calculated for the other performance metrics as follows,

$$\hat{\chi}_j = \frac{\chi_j - \chi_{min}}{\chi_{max} - \chi_{min}},$$
$$\hat{\nu}_j = \frac{\nu_j - \nu_{min}}{\nu_{max} - \nu_{min}}.$$

These normalized values ($\hat{\eta}$, $\hat{\chi}$, $\hat{\nu}$) are plotted for all the schedulers in Fig. 9. Note that an optimal scheduler has larger $\hat{\chi}$, smaller $\hat{\eta}$, and larger $\hat{\nu}$. From Fig. 9a, When $\alpha = 0$, the objective function minimizes the power consumption, and hence, the proposed scheduler achieves the least power consumption ($\hat{\eta} = 0$) among all the schedulers. Also, when $\alpha = 0$, the search space utilization of the proposed scheduler is better than the *Min-R_i* and *Max-R_i* scheduler. With increasing α, a better search space utilization is achieved at the cost of increased power consumption. When $\alpha = 1$, the objective function maximizes the search space utilization, and hence, the proposed scheduler achieves the best search space utilization ($\hat{\chi} = 1$). The power consumption of the proposed scheduler is still lesser than the *baseline*, *Max-R_i*, and *Max-R_i relaxed* schedulers. The *Min-R_i relaxed* scheduler has the highest $\hat{\chi}$ and the second lowest $\hat{\eta}$ among all the schedulers. However, the *Min-R_i relaxed* scheduler has poor fairness as shown in Fig. 9b, 9c. Note that by varying α, the proposed scheduler achieves various trade-offs between χ, η, and ν.

The baseline scheduler allocates only one IoT device in a search space in a round-robin fashion, and hence, has good fairness and search space utilization. However, the power consumption in the baseline scheduler is higher in comparison with the proposed scheduler (with any α), as shown in Fig. 6 and Lemma 2. Note that in NB-IoT, the devices are of low cost and limited by battery power. Additionally, since only one IoT device is scheduled per search space,

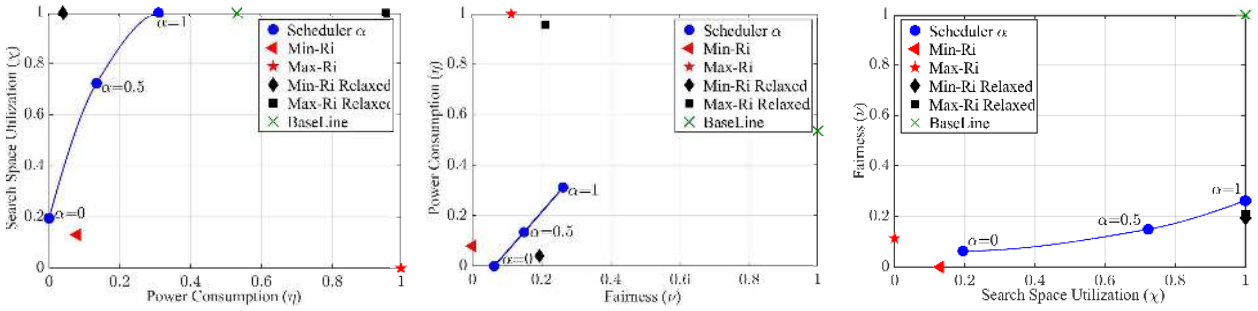

(a) Power Consumption $(\hat{\eta})$ *vs.* Search Space utilization $(\hat{\chi})$

(b) Fairness $(\hat{\nu})$ *vs.* Power Consumption $(\hat{\eta})$

(c) Search Space utilization $(\hat{\chi})$ *vs.* Fairness $(\hat{\nu})$

FIGURE 9. **Trade-off between various performance metrics normalized to a scale of [0, 1].**

the baseline scheduler results in a significant control signalling overhead, as the base station has to signal the search space region every time. Thus, the baseline scheduler is inefficient to implement in practice. Compared to the baseline scheduler, the sorting algorithms schedule more devices in each search space and are practically feasible in real-time. They have a better power consumption of the IoT devices when compared with the baseline scheduler.

When compared to all the schedulers, the proposed scheduler performs best in terms of power consumption (with $\alpha = 0$) and resource utilization of IoT devices (with $\alpha = 1$). With $\alpha = 0$, excluding the baseline scheduler, it is better than all the schedulers in terms of fairness of allocation. In real-time, when NB-IoT operates in in-band mode, the time-frequency resources are obtained from the cellular network and are valuable. Further, the NB-IoT devices have low battery capacity, and hence, the devices should have low power consumption. In such scenarios, with the proposed scheduler, the network operators can tune α to achieve desired trade-offs.

VII. CONCLUSION AND FUTURE WORK

We have proposed a novel resource mapping scheme for NB-IoT based on the uplink reference signals. We have also proposed a novel scheduler for NPDCCH and compared it with the existing control channel schedulers. With the proposed scheduler, the industrial operator can choose the parameters to address the requirements of power consumption of IoT devices, resource utilization, and fairness in service. Through Monte Carlo simulations, we have shown that the proposed scheduler achieves suitable trade-offs between various performance metrics. In the future, we will implement and validate the performance of the proposed schedulers on a hardware testbed.

REFERENCES

[1] *RAN1 Agreements for Rel-13 NB-IoT*, document TR TSG-RAN1, R1-161548, 3GPP, Ericsson, Feb. 2016.

[2] F. Tong, Y. Sun, and S. He, "On positioning performance for the narrowband Internet of Things: How participating eNBs impact?" *IEEE Trans. Ind. Informat.*, vol. 15, no. 1, pp. 423–433, Jan. 2019.

[3] *Physical Channels and Modulation*, document TS 36.211, 3GPP, Jul. 2016.

[4] *Physical Layer Procedures*, document TS 36.213, 3GPP, Jun. 2016.

[5] M. P. Reddy, G. Santosh, A. Kumar, and K. Kuchi, "Downlink control channel scheduling for 3GPP narrowband-IoT," in *Proc. IEEE 29th Annu. Int. Symp. Pers., Indoor Mobile Radio Commun. (PIMRC)*, Bologna, Italy, Sep. 2018, pp. 1–7.

[6] L. Feltrin, G. Tsoukaneri, M. Condoluci, C. Buratti, T. Mahmoodi, M. Dohler, and R. Verdone, "Narrowband IoT: A survey on downlink and uplink perspectives," *IEEE Wireless Commun.*, vol. 26, no. 1, pp. 78–86, Feb. 2019.

[7] S.-F. Cheng, "Multi-user scheduling for narrow band Internet of Things," in *Proc. SPACOMM*, Lisbon, Portugal, 2018, pp. 1–5.

[8] H. Malik, H. Pervaiz, M. M. Alam, Y. Le Moullec, A. Kuusik, and M. A. Imran, "Radio resource management scheme in NB-IoT systems," *IEEE Access*, vol. 6, pp. 15051–15064, 2018.

[9] N. Jiang, Y. Deng, A. Nallanathan, and J. A. Chambers, "Reinforcement learning for real-time optimization in NB-IoT networks," *IEEE J. Sel. Areas Commun.*, vol. 37, no. 6, pp. 1424–1440, Jun. 2019.

[10] C. Yu, L. Yu, Y. Wu, Y. He, and Q. Lu, "Uplink scheduling and link adaptation for narrowband Internet of Things systems," *IEEE Access*, vol. 5, pp. 1724–1734, 2017.

[11] V. Saxena, A. Wallen, T. Tirronen, H. S. Razaghi, J. Bergman, and Y. Blankenship, "On the achievable coverage and uplink capacity of machine-type communications (MTC) in LTE release 13," in *Proc. IEEE 84th Veh. Technol. Conf. (VTC-Fall)*, Montreal, QC, Canada, Sep. 2016, pp. 1–6.

[12] M. P. Reddy, G. Santosh, A. Kumar, and K. Kuchi, "Novel rate matching scheme for downlink control channel in 3GPP massive machine type communications," in *Proc. 10th Int. Conf. Commun. Syst. Netw. (COMSNETS)*, Jan. 2018, pp. 183–190.

[13] J. Hu, M. Wang, K. J. Zou, K. W. Yang, M. Hua, and J. Zhang, "Enhanced LTE physical downlink control channel design for machine-type communications," in *Proc. 7th Int. Conf. New Technol., Mobility Secur. (NTMS)*, Jul. 2015, pp. 1–5.

[14] V. Saxena, J. Bergman, Y. Blankenship, A. Wallen, and H. S. Razaghi, "Reducing the modem complexity and achieving deep coverage in LTE for machine-type communications," in *Proc. IEEE Global Commun. Conf. (GLOBECOM)*, Washington, DC, USA, Dec. 2016, pp. 1–7.

[15] T. P. C. de Andrade, C. A. Astudillo, and N. L. S. da Fonseca, "Allocation of control resources for machine-to-machine and human-to-human communications over LTE/LTE-A networks," *IEEE Internet Things J.*, vol. 3, no. 3, pp. 366–377, Jun. 2016.

[16] B. A. Salihu, D. Yang, X. Zhang, and S. Zubair, "New remapping strategy for PDCCH scheduling for LTE-advanced systems," *J. Commun.*, vol. 9, no. 7, pp. 563–571, 2014.

[17] Balamurali, "Optimal downlink control channel resource allocation for LTE systems," in *Proc. Int. Conf. Signal Process. Commun. (SPCOM)*, Bangalore, India, Jul. 2010, pp. 1–5.

[18] P. Hosein, "Resource allocation for the LTE physical downlink control channel," in *Proc. IEEE Globecom Workshops*, Nov. 2009, pp. 1–5.

[19] C. Karupongsiri, K. S. Munasinghe, and A. Jamalipour, "A novel random access mechanism for timely reliable communications for smart meters," *IEEE Trans. Ind. Informat.*, vol. 13, no. 6, pp. 3256–3264, Dec. 2017.

[20] Y. Chen, "Resource allocation for downlink control channel in LTE systems," in *Proc. 7th Int. Conf. Wireless Commun., Netw. Mobile Comput.*, Sep. 2011, pp. 1–4.
[21] C.-W. Huang, S.-C. Tseng, P. Lin, and Y. Kawamoto, "Radio resource scheduling for narrowband Internet of Things systems: A performance study," *IEEE Netw.*, vol. 33, no. 3, pp. 108–115, May 2019.
[22] Y.-J. Yu, "NPDCCH period adaptation and downlink scheduling for NB-IoT networks," *IEEE Internet Things J.*, early access, Jul. 20, 2020, doi: 10.1109/JIOT.2020.3010532.
[23] *Multiplexing and Channel Coding*, document TS 36.212, 3GPP, Jun. 2016.
[24] R. Bruno, A. Masaracchia, and A. Passarella, "Robust adaptive modulation and coding (AMC) selection in LTE systems using reinforcement learning," in *Proc. IEEE 80th Veh. Technol. Conf. (VTC-Fall)*, Vancouver, BC, Canada, Sep. 2014, pp. 1–6.
[25] *Study Channel Model for Frequencies from 0.5 to 100 GHz*, document TR 38.901, V 15.1.0, 3GPP, Sep. 2019.
[26] *Guidelines for Evaluation of Radio Interface Technologies for IMT-2020*, document ITU-R M.2412-0, ITU, Jul. 2017.
[27] *User Equipment (UE) Radio Transmission and Reception*, document TS 36.101, V 16.3.0, 3GPP, Sep. 2019.
[28] Q. Chen, G. Yu, R. Yin, A. Maaref, G. Y. Li, and A. Huang, "Energy efficiency optimization in licensed-assisted access," *IEEE J. Sel. Areas Commun.*, vol. 34, no. 4, pp. 723–734, Apr. 2016.
[29] M. R. Garey, R. L. Graham, and J. D. Ullman, "Worst-case analysis of memory allocation algorithms," in *Proc. 4th Annu. ACM Symp. Theory Comput. (STOC)*, 1972, pp. 143–150.
[30] G. Dósa and J. Sgall, "Optimal analysis of best fit bin packing," in *Automata, Languages, and Programming* (Lecture Notes in Computer Science), vol. 8572. Berlin, Germany: Springer, 2014, pp. 429–441, doi: 10.1007/978-3-662-43948-7_36.
[31] S. Umetani, M. Yagiura, and T. Ibaraki, "One-dimensional cutting stock problem with a given number of setups: A hybrid approach of metaheuristics and linear programming," *J. Math. Model. Algorithms*, vol. 5, no. 1, pp. 43–64, Apr. 2006.
[32] P. C. Gilmore and R. E. Gomory, "A linear programming approach to the cutting stock problem—Part II," *Oper. Res.*, vol. 11, no. 6, pp. 863–888, 1963.
[33] *AMPL*. Accessed: Sep. 23, 2020. [Online]. Available: https://ampl.com/products/solvers/open-source

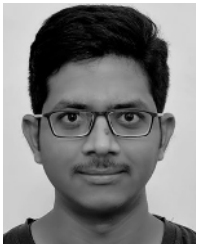

PAVAN REDDY MANNE received the M.Tech. degree in electrical engineering from IIT Hyderabad, Hyderabad, India, in 2018, where he is currently pursuing the Ph.D. degree. His research interests include physical-layer algorithms and the development of prototypes for fifth-generation systems. He was a recipient of the Excellence in Research Award at IIT Hyderabad in 2018.

SANTOSH GANJI (Graduate Student Member, IEEE) received the M.Tech. degree in electrical engineering from IIT Hyderabad, Hyderabad, India, in 2014. He is currently pursuing the Ph.D. degree with the Electrical and Computer Engineering Department, Texas A&M University, College Station, TX, USA. His research interests include in building the millimeter-wave communication systems, designing and building low power wide area networks, and directional medium access schemes.

ABHINAV KUMAR (Senior Member, IEEE) received the B.Tech. degree in electrical engineering and the M.Tech. degree in information and communication technology, and the Ph.D. degree in electrical engineering from IIT Delhi, in 2009 and 2013, respectively. In 2013, he was a Research Associate with IIT Delhi. From 2013 to 2014, he was a Postdoctoral Fellow with the University of Waterloo, Canada. Since 2014, he has been an Assistant Professor with IIT Hyderabad, Hyderabad, India. His current research interests include different aspects of wireless communications and networking.

KIRAN KUCHI (Member, IEEE) received the B.Tech. degree in electronics and communications engineering from Sri Venkateswara University College of Engineering, Tirupati, India, in 1995, and the M.S. and Ph.D. degrees in electrical engineering from The University of Texas at Arlington, Arlington, TX, USA, in 1997 and 2006, respectively. From 2000 to 2008, he was with Nokia Research, Irving, TX, USA, where he contributed to the development of a global system for mobile communication/EDGE, WiMax, and long-term evolution systems. From 2008 to 2011, he was with the Centre of Excellence in Wireless Technology, where he led fourth-generation research and standardization efforts. He was also an Adjunct Faculty with the Department of Electric Engineering, IIT Madras, Chennai, India. He is currently a Professor with the Department of Electrical Engineering, IIT Hyderabad, Hyderabad, India. He holds more than 20 U.S. patents. His current research interests include physical-layer algorithms and the development of prototypes for fifth-generation systems.